

Dynamic Behavior of Taipei 101 Tower: Field Measurement and Numerical Analysis

Q. S. Li, M.ASCE¹; Lun-Hai Zhi²; Alex Y. Tuan³; Chin-Sheng Kao⁴; Sheng-Chung Su⁵; and Chien-Fu Wu⁶

Abstract: This paper presents selected results measured from a monitoring system with 30 accelerometers installed at six floor levels in 508-m high Taipei 101 Tower located in Taipei City, Taiwan where earthquakes and strong typhoons are common occurrences. Emphasis is placed on analyzing the data recorded during three typhoons (Matsa, Talim, and Krosa) and a seismic event (Wenchuan earthquake occurred on May 12, 2008 in Shichuan, China) to investigate the effects of wind and seismic on the supertall building. Dynamic characteristics of the tall building such as natural frequencies, mode shapes, and damping ratios determined from the measured data are presented and compared with those calculated from the finite-element model of the high-rise structure. The seismic performance of this supertall building to a long distance earthquake (Wenchuan earthquake) is assessed based on the field measurements and numerical analysis. The findings of this study are expected to be of considerable interest and practical use to professionals and researchers involved in the design of supertall buildings.

DOI: 10.1061/(ASCE)ST.1943-541X.0000264

CE Database subject headings: Buildings, high-rise; Wind loads; Seismic effect; Finite element method; Numerical analysis; Measurement.

Author keywords: Tall building; Wind effect; Seismic effect; Dynamic characteristics; Finite-element method; Full-scale measurement.

Introduction

Due to the growing use of light weight and high-strength materials, modern tall buildings tend to be more flexible and lightly damped than those built in the past. As a result, these tall buildings are more sensitive to dynamic excitations by wind or seismic loads. It is thus required to investigate wind or seismic effects on such dynamic-sensitive structures. Generally, full-scale measurement is recognized as the most reliable way for evaluating dynamic behavior of tall buildings. In fact, monitoring dynamic effects on tall buildings can give practical validation of design procedures and assurance of acceptable behavior. Furthermore, field measurement results can be used to improve model test techniques and to refine the numerical models for structural analysis as well.

With the development of data acquisition techniques during the last three decades, a number of full-scale measurements of wind or seismic effects on tall buildings have been made through-

out the world (Jeary 1986; Ohkuma et al. 1991; Çelebi and Şafak 1992; Şafak and Çelebi 1992; Littler and Ellis 1992; Çelebi 1993; Tamura and Suganuma 1996; Li et al. 1998, 2004, 2005, 2006; Li and Wu 2004; Kijewski and Kareem 2001), including the measurement programs on four Chicago tall buildings currently being undertaken by Notre Dame University and the University of Western Ontario (Kijewski and Kareem 2001) and on 10 supertall buildings in Hong Kong and Mainland China by City University of Hong Kong (Li et al. 1998, 2004, 2005, 2006; Li and Wu 2004). However, as commented by Tamura et al. (2005), the chance to conduct full-scale measurements is quite rare, and obtained data are very important and valuable. In particular, literature review reveals that comprehensive full-scale measurements of wind or seismic effects on supertall buildings (building height >500 m) have never been conducted in the past. There is therefore a strong case for conducting such a study, since a number of supertall buildings are being designed and constructed around the world.

Taipei 101 Tower (shown in Fig. 1) is located in Hsinyi District, Taipei, Taiwan. When the construction of the tall building was completed in 2003, it was the world's tallest building. The superstructure is a 101-story office tower with five additional basement levels going down to -19.4 mPD and is of height 508 mPD. The general footprint of the building is about 45.9 × 45.9 m and the gross floor area is about 180,000 m² with 4.2-m typical floor-to-floor height. The aspect ratio of the building's height to its transverse width is about 10. For such a tall and slender high-rise structure located in a region well known for extreme typhoons and earthquakes, current codes and standards may not be adequate to cover its design. These features warrant a detailed study on the structural performance especially its dynamic behavior. The findings of such a study will certainly be valuable for design and construction of other supertall buildings in the future.

¹Associate Professor, Dept. of Building and Construction, City Univ. of Hong Kong, Kowloon, Hong Kong (corresponding author). E-mail:bcqsli@cityu.edu.hk

²Ph.D. Candidate, College of Civil Engineering, Hunan Univ., Changsha, Hunan 410082, China.

³Assistant Professor, Dept. of Civil Engineering, Tamkang Univ., Tamsui, Taiwan.

⁴Associate Professor, Dept. of Civil Engineering, Tamkang Univ., Tamsui, Taiwan.

⁵Junior Technical Specialist, Central Weather Bureau, Taipei, Taiwan.

⁶Chief, Central Weather Bureau, Taipei, Taiwan.

Note. This manuscript was submitted on December 23, 2009; approved on June 6, 2010; published online on June 15, 2010. Discussion period open until June 1, 2011; separate discussions must be submitted for individual papers. This paper is part of the *Journal of Structural Engineering*, Vol. 137, No. 1, January 1, 2011. ©ASCE, ISSN 0733-9445/2011/1-143-155/\$25.00.



Fig. 1. Elevation view of Taipei 101 Tower

To evaluate the performance of the supertall building under typhoon and earthquake actions, a monitoring system was installed in the building, including 30 accelerometers at six different floor levels in the building. Significant field data have been acquired from the instrumented tower over the last several years, including measurements made during the passage of several typhoons and under earthquake excitations. This paper presents selected results of the data analysis based on the measurements made during three typhoons and a recent seismic event. Furthermore, the measured data are also used to compare with numerical results for improvement of numerical modeling and development of design guidelines. The main objective of this study is to further the understanding of wind and seismic effects on supertall buildings as well as to apply such knowledge to design.

Structure and Monitoring System

Taipei 101 Tower is a composite steel/concrete structure. A pinnacle on top of the 448-m high building brings the total height to 508 m. The superstructure contains a steel frame with H-shape steel beams and composite floors, constructed with concrete slabs and metal decks (Research Institute of Building and Construction 2003). Belt trusses, one or two-story high, are placed every eight-story interval at the perimeter frame, and the brace core is con-

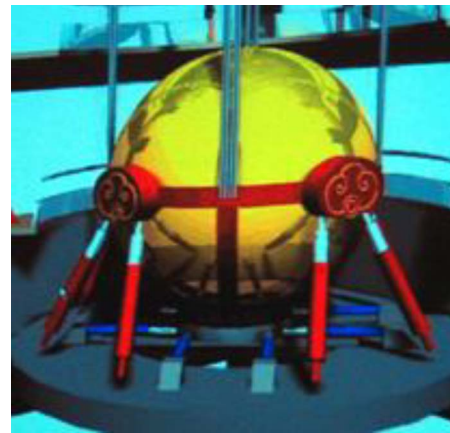


Fig. 2. Photo of the 660-t TMD installed in Taipei 101 Tower

nected to megacolumns via belt trusses consisting of in-floor braces and vertical trusses. The structure is a dual system: the external structure is composed of the megacolumns and external columns providing the lateral rigidity to the seismic and wind loads, and the internal structure, also designated as substructures, provides the available spaces and allows for significant amount of energy dissipation. In addition, a tuned mass damper (TMD) made of steel with a diameter of 6 m and weighing 660 t, the largest of its kind in the world, has been installed in Floors 87–91, which is essentially a pendulum that spans five floors (as shown in Fig. 2). Two ingenious compact TMDs have been placed within the uppermost 8 m of the pinnacle. The primary function of these TMDs is to suppress wind-induced vibrations. Meanwhile, they were designed to withstand the forces generated in a strong seismic event with up to a 2,500-year return period (Research Institute of Building and Construction 2003). The tall building is surrounded by a number of buildings including some tall buildings with a height of more than 100 m. The site around the building can be regarded as an urban terrain.

The monitoring system installed in Taipei 101 Tower includes two major parts: the data acquisition and storage platform, sensor subsystem. Sensor subsystem includes 30 wired accelerometers (TS AS-2000C) which are located at the -5th (basement), 1st, 36th, 60th, 89th, and 101st floor as shown in Fig. 3. In order to measure the rotational accelerations of the tower, several accelerometers were placed at two locations on a floor along the two major orthogonal axes (directions X and Y) of this building, as shown in Fig. 4. Acceleration responses from the tall building were continuously acquired and digitized at 200 Hz by a high-resolution digital data logger (TS SAMTAC-700). Through the analysis of the data measured from these sensors, structural acceleration responses and dynamic characteristics (such as natural frequencies, mode shapes, and damping ratios) of the tall building can be obtained.

The acceleration data presented in this paper were measured during a 34-month period from August 2005 to May 2008. Emphasis was placed on analyzing the data recorded during three typhoons (Matsa, Talim, and Krosa) and a seismic event (Wenchuan earthquake occurred on May 12, 2008 in Shichuan, China). Table 1 presents the relevant information on the typhoons.

Modal Identification Techniques

Structural modal parameter identification based on ambient vibrations measurements has received considerable attention in the

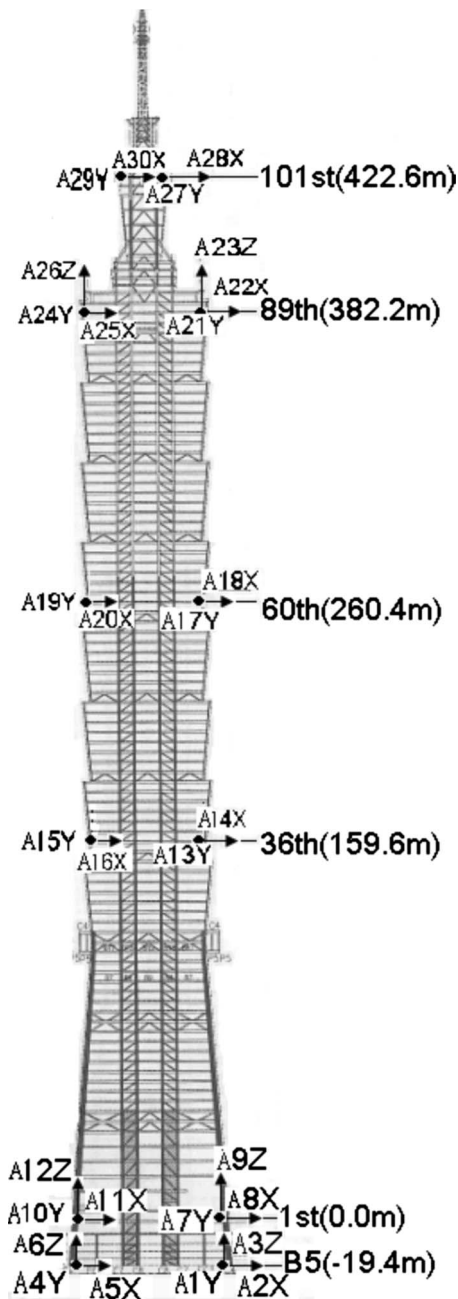


Fig. 3. Elevation and locations of the installed accelerometers

civil engineering community in recent years (Ivanovic et al. 2000; Brownjohn 2003; Kim et al. 2005). There are several techniques to identify “natural” modes of a structure. In this research, three methods were used to extract the modal parameters from the dynamic measurements.

PP Method

A fast method to estimate the modal parameters of a structure subjected to ambient excitations is the so-called peak-picking (PP) method. The method is named after the key step of the method: the identification of the eigenfrequencies as the peaks of a spectrum plot. The method is described in detail in Bendat and Piersol (1993), Andersen et al. (1999), and Peeters and Roeck (2001). Under the conditions of low damping and well-separated eigenfrequencies, the natural frequencies of a structure can be

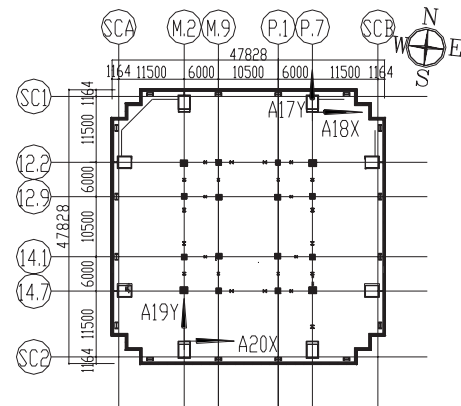


Fig. 4. Accelerometer arrangement on the 60th floor

determined by taking the peaks of the response spectrum. Due to its simplicity in implementation: the only algorithm that is needed is the fast Fourier transform (FFT) to convert time data to a spectrum; the method is very popular and has been used successfully for a large amount of structures.

FDD Method

The frequency domain decomposition (FDD) method is an extension of the PP method (Brincker et al. 2001; Michel et al. 2008; Magalhaes et al. 2010). The first step of this method is to estimate the spectral matrix of the ambient responses. The spectral matrix is decomposed at discrete frequencies $\omega = \omega_i$ using singular value decomposition

$$G_{yy}(j\omega_i) = U_i S_i U_i^H \quad (1)$$

where the matrix $U_i = [u_{i1}, u_{i2}, \dots, u_{im}]$ = matrix of the singular vectors and S_i = diagonal matrix of the scalar singular values. Close to a peak corresponding to the k -th mode in the spectrum, only the k -th mode is dominant, and the power spectral density (PSD) matrix approximates to a rank-one matrix and can be decomposed as

$$G_{yy}(j\omega_i) = u_{i1} s_{i1} u_{i1}^H \quad \omega_i \rightarrow \omega_k \quad (2)$$

Thus, the first singular vector u_{i1} is an estimate of the mode shape at that frequency and the first singular value is autospectral density function of a single degree of freedom (SDOF) system with the same frequency and damping as the structural vibration mode. This PSD function is identified around the peak by comparing the mode shape estimate with the singular vectors for the frequency lines around the peak. In order to identify the PSD function of the SDOF system, the modal assurance criterion (MAC) is adopted and is defined as (Allemang and Brown 1982)

Table 1. Maximum Gust Speed Recorded at Taipei Meteorological Observation Station

Typhoons	Date	Wind direction	Maximum gust (m/s)
Masta	August 5, 2005	NW	28.5
Talim	August 31, 2005	NE	36.3

Note: [Taipei Meteorological Observation Station is located at 25°02'15.0"N, 121°30'52.1"E; measurement height (location of the anemometer) is 33.8 m from the ground].

Table 2. Natural Frequencies of Sway Modes

		Direction X			Direction Y		
		Mode 1 (Hz)	Mode 2 (Hz)	Mode 3 (Hz)	Mode 1 (Hz)	Mode 2 (Hz)	Mode 3 (Hz)
PP ^a	Masta	0.156	0.440	0.801	0.147	0.435	0.783
	Talim	0.156	0.439	0.788	0.147	0.432	0.781
	Krosa	0.147	0.430	0.772	0.146	0.420	0.762
	Wenchuan	0.147	0.430	0.781	0.145	0.425	0.772
FDD	Masta	0.153	0.436	0.784	0.151	0.433	0.781
	Talim	0.152	0.434	0.785	0.150	0.426	0.778
	Krosa	0.150	0.426	0.768	0.149	0.420	0.778
	Wenchuan	0.148	0.425	0.785	0.147	0.420	0.762

^aResults determined by the PP method are the overall average values of the natural frequencies measured from the accelerometers located at six-story levels.

$$\text{MAC}(\phi_i^A, \phi_i^B) = \frac{[(\phi_i^A)^T \phi_i^B]^2}{[(\phi_i^A)^T \phi_i^A][(\phi_i^B)^T \phi_i^B]} \quad (3)$$

where $\phi_i^A = i$ th measured mode shape vector and $\phi_i^B = i$ th mode shape vector at the surrounding frequencies, respectively. As long as a high MAC value (usually 0.8) is found between the shape at one frequency and the shape at the peak, we consider that the corresponding singular value belongs to the SDOF density function. From the identified SDOF density function, an autocorrelation function can be calculated by applying an inverse FFT to the autospectral density function. Then, the natural frequency and the damping can be obtained by estimating crossing times and the logarithmic decrement of the corresponding SDOF autocorrelation function.

RDT

The random decrement technique (RDT) represents a quick and practical method for establishing the nonlinear damping characteristics (Tamura and Suganuma 1996; Glanville et al. 1996; Li et al. 1998, 2004, 2005; Campbell et al. 2007; Pirnia et al. 2007). The determination of the amplitude-dependent damping ratios for a building included the following steps:

1. In order to obtain the damping ratio of each mode, the measured signals of the stationary response data are band-pass filtered before processing the random decrement technique to remove the components not concerned.
2. There are several ways to achieve the random decrement signatures. In this study, a set of thresholds are used to find segments for obtaining a set of random decrement signatures with different initial amplitudes.
3. Regarding the random decrement signature as a free vibration signal, the damping ratio is determined using the least-squares approximation accordingly.

Dynamic Characteristics and Structural Responses

Natural Frequency

The results of spectral analysis of the acceleration responses measured from the accelerometers located at several story levels in Taipei 101 Tower are shown in Tables 2 and 3. These spectra were obtained from a direct analysis of the accelerations measured during the typhoons and the Wenchuan earthquake. The spectral analysis results show that the acceleration responses of the super-tall building were primarily in the two fundamental sway modes of vibration, but higher modes were also clearly present. Meanwhile, rotational modes of the building were also identified based on the acceleration responses data which were measured from four accelerometers placed at two locations on the same floor. The natural frequencies were also estimated by the FDD method as shown in these tables. The singular values of the decomposed spectral matrix are shown in Fig. 5. The first several modes are easily identified in both plots. The natural frequencies measured from Taipei 101 Tower during Typhoon Krosa and the Wenchuan earthquake (corresponding to relatively larger vibration amplitudes) were lower than those determined based on the measurements during Typhoons Matsa and Talim. This can be attributed to the differences of the measured vibration amplitudes during the three typhoons and the earthquake, indicating that the natural frequencies decreased as the vibration amplitude became larger. The estimates of natural frequencies obtained by the PP method and the FDD method were in good agreement.

Natural frequency is one of the most important parameters for describing the dynamic characteristics of a tall building. Accurate determination of natural frequencies is essential to correctly predict wind-induced acceleration for serviceability assessments in the design of tall buildings. Ellis (1980) proposed an approximation for the fundamental frequency $f_1 = 46/H$ (where the unit of f_1

Table 3. Natural Frequencies of Rotational Modes

	PP				FDD			
	Masta	Talim	Krosa	Wenchuan	Masta	Talim	Krosa	Wenchuan
Mode 1 (Hz)	0.249	0.244	0.234	0.240	0.247	0.246	0.229	0.231
Mode 2 (Hz)	0.596	0.605	0.571	0.586	0.594	0.596	0.573	0.591

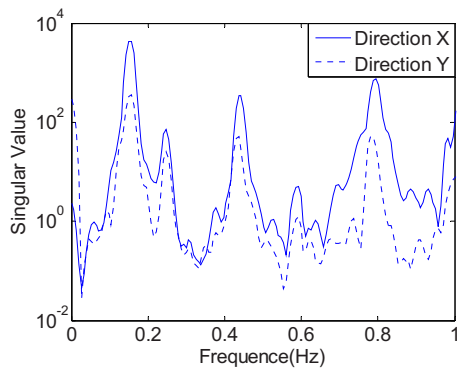


Fig. 5. Singular values of the PSD matrix during Typhoon Matsa

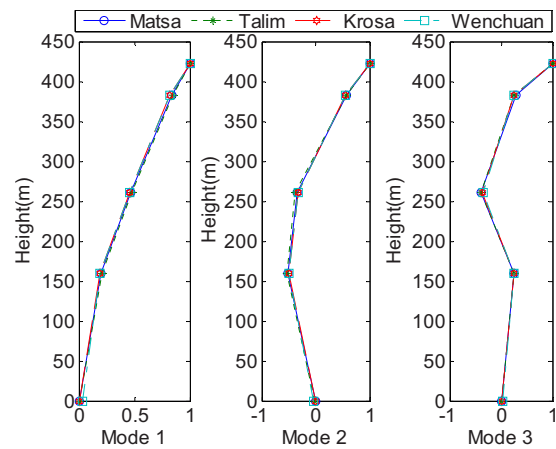
and H is hertz and meters, respectively) for all types of buildings, which has been used in several codes and standards such as the Code of Practice on Wind Effects in Hong Kong (Buildings Department of the Government of the Hong Kong SAR 2004), and the Australian and New Zealand Standard AS/NZS 1170.2 (Standards Australia and Standards New Zealand 2002). Recently, Tamura et al. (2000) suggested an empirical expression $f_1 = 67/H$ for steel encased reinforced concrete (SRC) buildings, based on field measurements taken in Japan. The empirical formula recommended by Tamura et al. gives a higher natural frequency than Ellis' proposal. In this study, as the structure height of Taipei 101 Tower is about 448 m from the ground, the calculated value of the fundamental frequency from the two equations by Ellis and Tamura is 0.103 and 0.150 Hz, respectively, while the measured values during the three typhoons and the Wenchuan earthquake were in the range of 0.145–0.147 Hz. The measured natural frequencies of the SRC-building are in better agreement with the empirical value suggested by Tamura et al.

Mode Shape Estimation

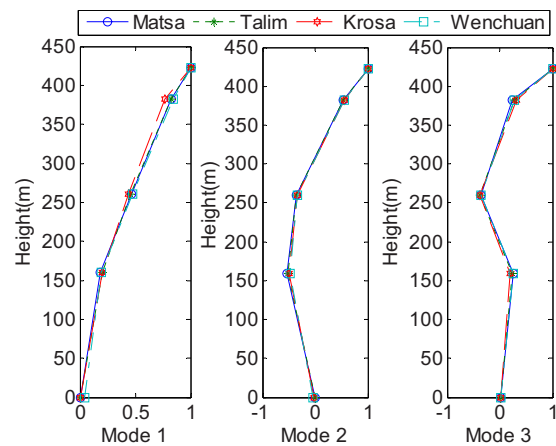
As introduced previously, 30 accelerometers were employed to measure the dynamic responses which can be used to identify the mode shapes of Taipei 101 Tower. The records of the six accelerometers located at the -5 th floor in the basement were considered as reference data for the determination of the mode shapes. Figs. 6(a and b) show the first three sway mode shapes in directions X and Y , respectively, determined from the acceleration responses measured during the three typhoons and the Wenchuan earthquake. The mode shapes presented in this paper were normalized to $\Phi=1$ at the 101st floor for each mode. It can be seen from these figures that the measured mode shapes during the three typhoons and the Wenchuan earthquake are very similar, implying that the determined mode shapes are reliable. In addition, the first sway mode shape curves in both directions clearly demonstrate nonlinear variations with the building height, i.e., the bending deformation, is dominant in the total deformations. This is contrary to the assumption of a linear distribution for the first sway mode shape adopted in some existing codes and standards as well as in force measurements in wind tunnel tests. From Fig. 6, it appears that the assumption may result in errors in the estimation of equivalent static wind loads and responses of tall buildings on the basis of force measurement results from wind tunnel tests.

Damping Estimation

In general, the dynamic response of a structural system is greatly affected by the amount of damping in each mode of vibration.



(a) Direction X



(b) Direction

Fig. 6. Mode shapes of sway modes measured from the Taipei 101 Tower

The importance of damping is becoming increasingly significant as modern tall buildings are becoming taller and more flexible. However, as yet, there is no widely accepted method available for estimating damping ratios of a structure prior to construction. Reliable evaluations of structural damping can be obtained from field measurements of a prototype building only.

In this study, the measured acceleration data were used to obtain the damping estimates. The overall damping ratios, as shown in Table 4, which actually comprise of both structural damping and aerodynamic damping, were determined by the FDD method and the random decrement technique based on the field data; while the damping ratios of the first two rotational modes estimated by the FDD are given in Table 5. Table 4 shows that damping ratios identified by the FDD are basically consistent with those determined by the RDT. It is also observed that the damping ratios in the first sway mode in both directions X and Y are greater than those of the higher modes. Table 5 indicates that the variation of damping ratios of the rotational modes is relatively small, which may be attributed to the relatively small rotational response of the square building during the typhoons and the earthquake. Furthermore, the measured overall damping ratios of the building under typhoon conditions are found to be larger than those measured from other tall buildings having similar structural systems but lower heights (Li et al. 2004, 2005), especially for the first mode along the two orthogonal directions during Typhoon Krosa.

Table 4. Damping Ratios of Taipei 101 Tower (Sway Modes)

		Direction X			Direction Y		
		Mode 1 (%)	Mode 2 (%)	Mode 3 (%)	Mode 1 (%)	Mode 2 (%)	Mode 3 (%)
FDD	Masta	1.63	0.98	0.73	1.4	1.1	0.59
	Talim	1.00	0.73	0.59	0.98	1.1	0.62
	Krosa	3.74	1.82	0.98	2.46	1.5	0.89
	Wenchuan	2.41	2.22	1.6	2.15	1.52	0.88
RDT ^a	Masta	1.34	0.74	0.67	1.04	1.33	0.50
	Talim	0.77	0.52	0.6	0.82	0.94	0.44

^aResults determined by the RDT are the overall average values of the damping ratios measured from the accelerometers located at six story levels.

These differences may be attributed to several reasons, including the relatively large vibration amplitudes of Taipei 101 Tower and the existence of the TMD installed on the Floors 87–91.

The information on the amplitude-dependent damping ratio obtained from Taipei 101 Tower is very valuable since similar measurements are rare in the literature. Fig. 7 shows the variation of the damping ratios determined by the FDD method with the peak acceleration responses measured atop the building (the 101st floor) during the typhoons and the earthquake. It can be seen from the figure that there is a tendency for the damping ratios of the first three sway modes in both directions X and Y increase with the increases in vibration amplitude. In order to further understanding of the characteristics of the amplitude-dependent damping of the tall building, the variations of damping ratios against vibration amplitude for the first three sway modes in the two directions were determined by the random decrement technique. Damping ratios determined from the records of four accelerometers located on the 101st floor during Typhoons Matsa and Talim are presented in Fig. 8. It is evident that the damping curves

demonstrate nonlinear energy dissipation characteristics.

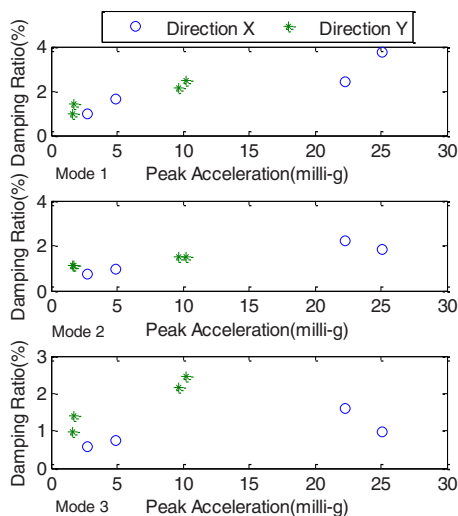
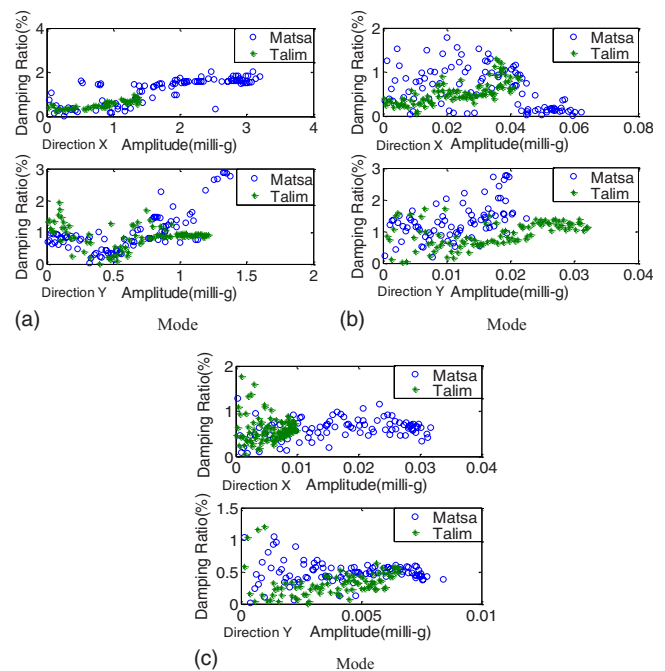
From the measurements of damping, it is found that the amplitude-dependent damping ratios of the fundamental modes in the two orthogonal directions varied in the range of 0.77–3.74% during the typhoons and the earthquake. It appears that damping values of 1.0–2.0% for the low vibration amplitude range (peak acceleration response < 10 mg) and 2–4% for the higher vibration amplitude level (peak acceleration response > 10 mg) of critical are reasonable for the wind-resistant analysis of the super-tall building for serviceability consideration.

Correlation of Numerical Results and Field Measurements

A three-dimensional (3D) finite-element (FE) model of Taipei 101 Tower structure, as shown in Fig. 9, was established based on the structural design drawings. Four kinds of elements were employed in establishing the FE model: 12-nodes 3D beam elements, suitable for nonlinear large rotations and large strains, were employed to model columns and beams. 3D link elements were used to model braces. Mass elements were employed to model the live loads and nonstructural components. The floors

Table 5. Damping Ratios of Rotational Modes (FDD Method)

	Masta	Talim	Krosa	Wenchuan
Mode 1 (%)	1.1	1.2	1.29	1.4
Mode 2 (%)	0.95	0.88	0.81	1.1

**Fig. 7.** Variation of damping ratios against peak acceleration response (at Floor 101) for the first three sway modes during the typhoons and the earthquake**Fig. 8.** Variation of damping ratio with vibration amplitude at the Floor 101 during the typhoons

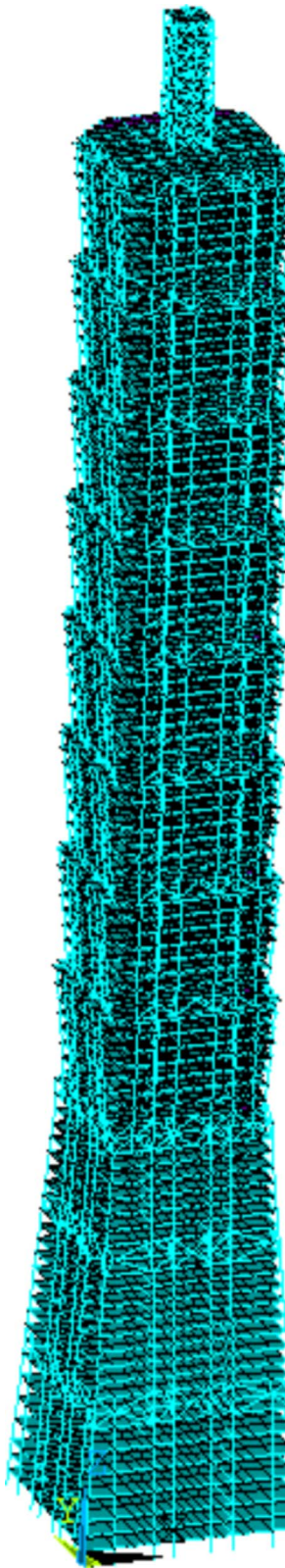


Fig. 9. FE model of Taipei 101 Tower

were modeled with shell elements. The connection between the structure and its foundation was treated to be fixed. The first five natural frequencies and mode shapes determined by the FE model, including two modes for translational motions in each horizontal direction and one mode for rotational motion about the vertical axis, are shown in Table 6 and Fig. 10, respectively. For

comparison purposes, the overall average values of the natural frequencies measured during the typhoons and the earthquake and the differences between the calculated and measured natural frequencies for the first five modes are listed in Table 6. There are about -7.4 to 15.7% differences between the two sets of results. The measured results are all larger than the calculated ones except the rotational mode. The differences between the calculated and measured natural frequencies can be attributable to several reasons, including that the effective mass values of the building are less than those assumed at the design stage, and/or the effective stiffness values of the building are higher than those determined at the design stage due to the contribution of nonstructural components.

In order to determine the correlation between the mode shapes of the FE analysis and from the measurements, the MAC and the normalized modal difference (NMD) (Waters 1995) are adopted to identify the correlations between a pair of mode shape vectors. The NMD is defined as

$$\text{NMD}(\phi_i^A, \phi_i^B) = \sqrt{\frac{1 - \text{MAC}(\phi_i^A, \phi_i^B)}{\text{MAC}(\phi_i^A, \phi_i^B)}} \quad (4)$$

The MAC is a dimensionless quantity and ranges from 0 to 1. The case of $\text{MAC}=1$ corresponds to perfect correlation of the two mode shape vectors, while $\text{MAC}=0$ represents uncorrelated vectors. In general, a MAC value greater than 0.80 is considered as a good match, while a MAC value less than 0.40 is regarded as a poor match. On the other hand, the NMD is a close estimate of the average difference between a calculated mode shape vector and a measured mode shape vector, which is more sensitive to mode shape differences than MAC (Li and Wu 2004). A smaller NMD value indicates a better correlation for the two mode shape vectors. Table 7 lists the values of the MAC and NMD of the measured and calculated sway mode shapes. It is observed that there is a good correlation between the measured and calculated mode shapes in both directions, while the lower modes show better correlation than the higher modes.

Seismic Analyses

Dynamic response by seismic loads is one of the most important design criteria for tall buildings. Previous studies (Pan 1995; Tao and Brownjohn 1998; Brownjohn et al. 2000; Brownjohn and Pan 2001; Pan et al. 2004; Fan et al. 2009) showed that the dynamic responses of tall buildings due to long-distance earthquakes may be greater than those caused by strong winds. The characteristic long-period waves of a distant earthquake could potentially cause damages to or large vibrations of long-period sensitive structures such as supertall buildings. Thus, the investigation of the dynamic responses of Taipei 101 Tower under a long-distance earthquake excitation may provide useful information for the design of supertall buildings in the future.

On May 12, 2008, a devastating earthquake (Wenchuan earthquake) took place at 02:28 p.m. local time in Sichuan Province of the People's Republic of China, about 1,900 km away from Taipei. The China Earthquake Administration (2008) estimated the magnitude of the event as M_s 8.0, with a focal depth of 14 km. A set of strong-motion acceleration responses of Taipei 101 Tower under the Wenchuan earthquake was recorded by the monitoring system installed in the building, which will be analyzed and presented below.

Table 6. Measured and Calculated Natural Frequencies

Modes	Sway modes				
	Direction X		Direction Y		Rotational mode, Mode 1 (Hz)
	Mode 1 (Hz)	Mode 2 (Hz)	Mode 1 (Hz)	Mode 2 (Hz)	
Calculated (Hz)	0.134	0.370	0.133	0.361	0.260
Measured (Hz)	0.152	0.435	0.146	0.428	0.242
Difference (%) ^a	11.8	14.9	8.9	15.7	-7.4

^aDifference=(measured-calculated)/measured.

Earthquake Record Data at the Basement

The rigidity of the building’s concrete pile-supported mat foundation is large, indicated by a small modal ordinate at the basement level shown in Fig. 6. Then, the acceleration responses recorded at the -5th floor in the basement (B5) were used as the input to the 3D FE model of the Taipei 101 Tower for the time-history analyses of the structural seismic responses.

The raw acceleration response data recorded at the B5 during the Wenchuan earthquake are shown in Fig. 11. The recorded peak accelerations in directions X, Y, and Z were 1.32, 1.17, and 0.6 mg, respectively, which show that the measured accelerations are larger in directions X and Y (horizontal) than direction Z (vertical). The power spectral densities of the accelerations at the basement are shown in Fig. 12. It appears that most of the high-frequency components of the earthquake wave would have been filtered out by the earth during the long-distance travel, and that

the accelerations at the Taipei 101 site mainly contained frequencies lower than 1 Hz. Under such an earthquake excitation, the fundamental mode responses were more predominant than higher mode responses.

Amplitude Spectral Ratio

The amplitude spectral ratios or the transfer functions of the acceleration responses recorded at the 1st, 36th, 60th, 89th, and

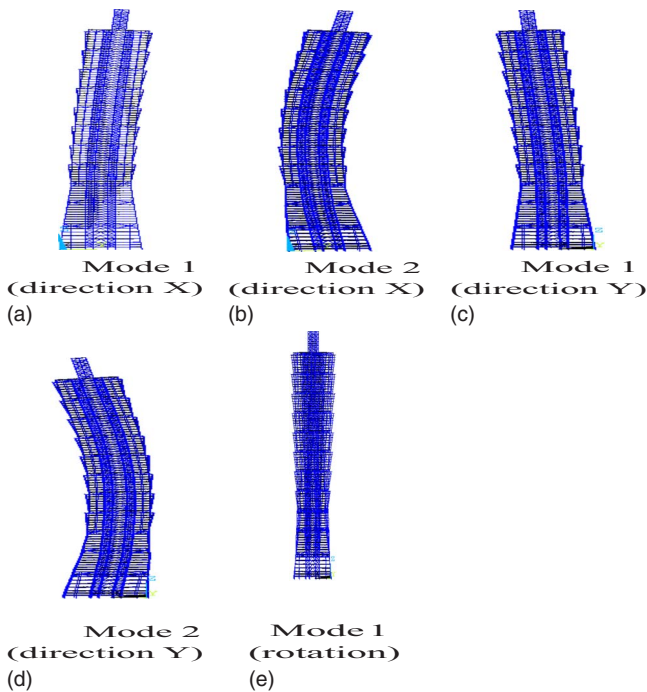


Fig. 10. Calculated mode shapes of Taipei 101 Tower

Table 7. Correlation Index of the Measured and Calculated Mode Shapes

Mode	Direction X		Direction Y	
	Mode 1	Mode 2	Mode 1	Mode 2
MAC	0.995	0.980	0.996	0.976
NMD (%)	7.1	14.4	6.3	15.8

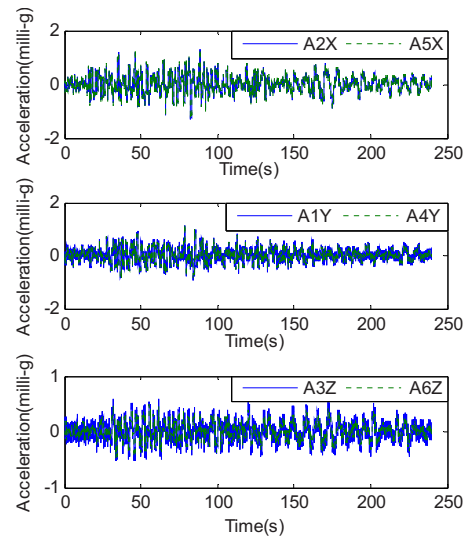


Fig. 11. Time histories of acceleration responses at basement (B5) during Wenchuan earthquake

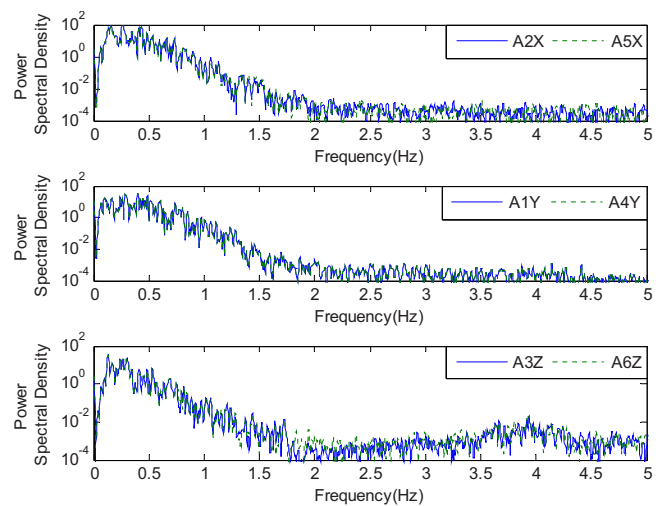


Fig. 12. Power spectral densities of the accelerations at the basement (B5) during Wenchuan earthquake

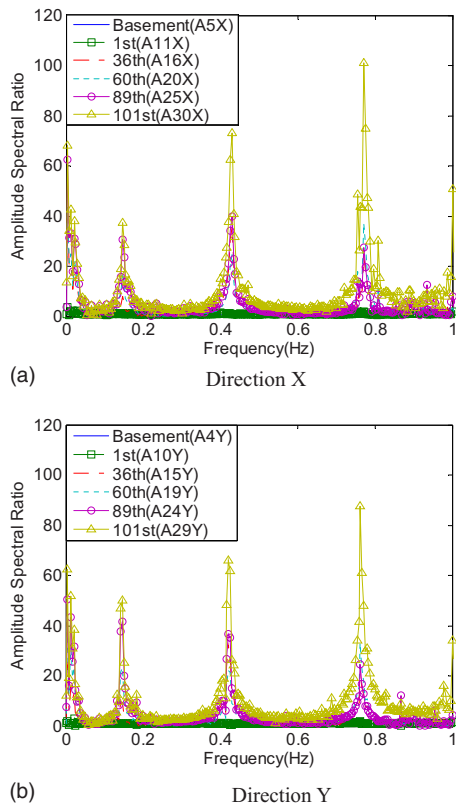


Fig. 13. Amplitude spectral ratio of the accelerations at the 1st, 36th, 60th, 89th, and 101st floors to the basement acceleration

101st floor to the basement accelerations are shown in Fig. 13. Compared with the acceleration response data at the basement (B5), the dynamic responses of the high-rise structure at other instrumented floor levels were significantly amplified under the seismic excitation. The floor amplitude spectral ratios corresponding to the first three sway modes in directions *X* and *Y* during the Wenchuan earthquake are given in Table 8. It is seen that the amplitude spectral ratios for the fundamental sway modes in the two orthogonal directions increase with the increasing building height. However, the ratios for the second and the third modes in the two directions do not always increase with the increasing building height. Furthermore, it also appears that the amplitude spectral ratios at the 101st floor corresponding to the first three sway modes in both directions are much larger than those obtained on the other five levels. This may be attributed to the smaller floor area and rigidity of the 101st floor.

Table 8. Amplitude Spectral Ratios during Wenchuan Earthquake

Floor		B5 (basement)	1st	36th	60th	89th	101st
Direction <i>X</i>	Mode 1	1.00	1.12	7.79	17.59	30.60	37.43
	Mode 2	1.00	1.01	35.53	24.49	39.97	73.11
	Mode 3	1.00	2.01	23.87	36.94	27.26	101.16
Direction <i>Y</i>	Mode 1	1.00	1.04	9.24	23.21	41.57	50.17
	Mode 2	1.00	1.24	32.14	21.95	36.52	66.09
	Mode 3	1.00	1.82	21.43	32.97	24.62	87.77

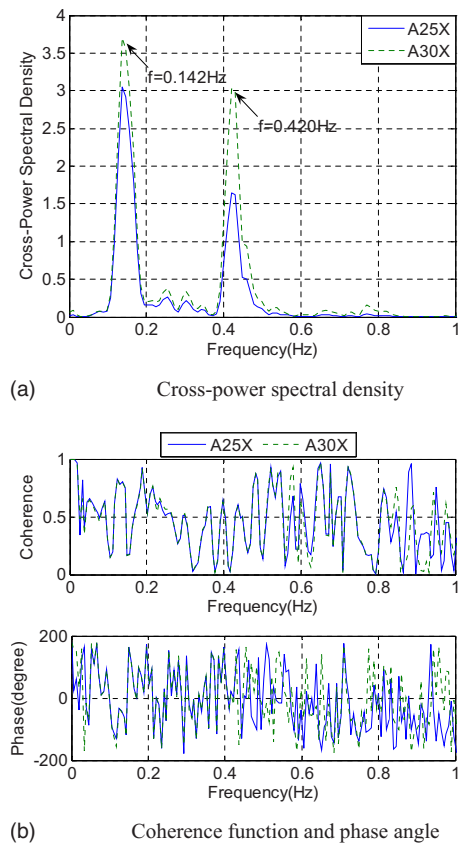


Fig. 14. Cross PSD, coherence function, and phase angle of the vertical acceleration at the basement (B5) with the accelerations in the *X* direction at the 89th and 101st floors

Rocking Motions

In order to identify the existence of rocking motion of the building, the cross spectra, coherence function, and phase angle, between the horizontal acceleration at the 101st floor and the vertical motion in the basement, were calculated and are shown in Figs. 14 and 15. The cross spectra clearly show two amplitudes in each direction. Even though the motions have near-zero phase angles at these frequencies, the coherences are very low. Therefore, the rocking motions are insignificant and can be neglected. This is not surprising since the building is supported by a pile foundation.

Time-History Analysis

Time-history analysis is an effective dynamic analysis method to investigate the seismic performance of tall buildings. It can pro-

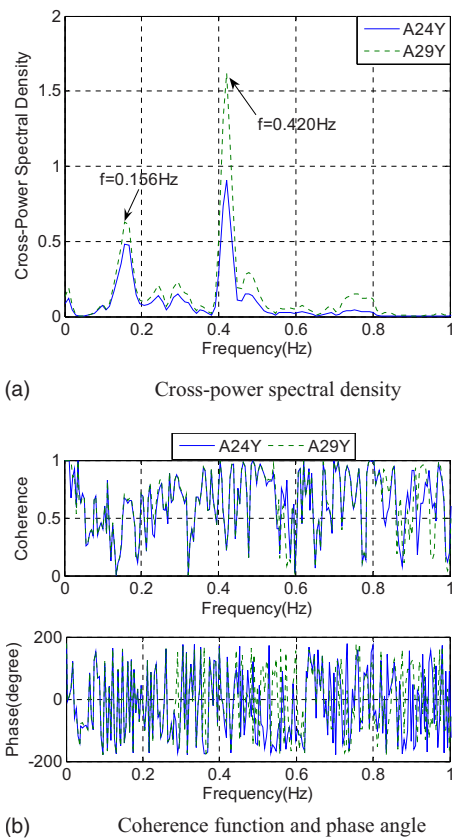


Fig. 15. Cross PSD, coherence function, and phase angle of the vertical acceleration at the basement (B5) with the accelerations in the Y direction at the 89th and 101st floors

vide useful information for the earthquake-resistant design and the design of active and passive control devices for reduction of structural vibrations. The approach is composed of a step-by-step direct integration, in which the time domain is discretized into a large number of small increments, and the equations of motion are solved for each time interval to obtain the structural responses such as accelerations and displacements, etc. In this study, the accelerations recorded by accelerometers 1Y, 2X, and 3Z at the basement (B5) during the Wenchuan earthquake were selected as input for the time-history analysis. The modal damping ratios were selected based on the measured results during the earthquake, as shown in Tables 4 and 5. The measured damping ratios for the first two sway modes of the building in both directions were in the range between 2.15 and 2.4% except for the second mode in direction Y. The averaged value of 2.26% was used for all modes of the tall building in the present dynamic analysis.

The time histories of the recorded and the calculated acceleration responses at the 89th floor and the 101st floor in both directions X and Y are compared in Fig. 16. It is observed that the simulated acceleration responses fit those recorded by the accelerometers on the P.7 axis (see Fig. 4) well. Meanwhile, the calculated acceleration responses are also in good agreement with the data measured by the accelerometers on the M.2 axis (see Fig. 4). It is found that the rotational acceleration responses were not obvious. The maximum values of the recorded and the simulated acceleration responses at the 89th and 101st floors are given in Table 9 for comparison purposes. The simulated maximum accelerations correlate with the recorded data well. The good agreement between the calculated results and the measured data

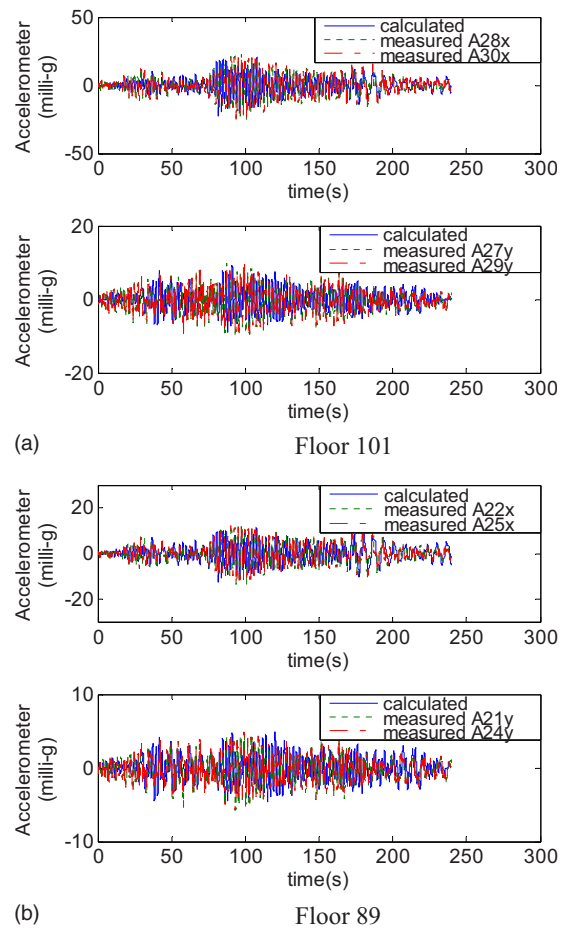


Fig. 16. Comparison of the time histories of acceleration responses at the 89th and 101st floors in directions X and Y

indicates that the dynamic analysis with the FEM can satisfactorily predict the seismic performance of the supertall building.

The dynamic amplification factors of the high-rise structure in directions X and Y under the excitation of the Wenchuan earthquake are shown in Fig. 17. The calculated dynamic magnification factors of the building in both directions agree with the measured results well. Below the 36th story level, the calculated and measured dynamic magnification factors in both directions gradually increased with the building height. However, the dynamic magnification factors decrease with the increase of the building height from the 36th to 80th stories. Above the 80th floor, especially from the 91st to 101st stories, the dynamic magnification factors in both directions increase with the building height. The computational results as well as the measurements of the dynamic magnification factors demonstrate that the supertall

Table 9. Measured and Calculated Peak Acceleration Responses

Floor	Direction X (mg)		Direction Y (mg)	
	Calculated	Measured	Calculated	Measured
1st	1.19	1.31	1.02	1.16
36th	9.37	10.5	4.57	4.4
60th	7.21	7.99	4.42	3.2
89th	11.18	13.1	4.94	5.05
101st	20.14	22.1	9.31	9.68

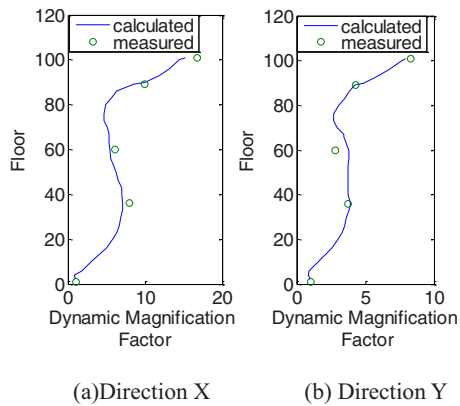


Fig. 17. Dynamic magnification factors

building was sensitive to dynamic excitations by such a long-distance earthquake. The long-period wave characteristics of such a distant earthquake have significant influences on the dynamic responses of the tall building, even if the ground acceleration amplitude was relatively small. The dynamic responses at the upper stories of the high-rise structure were significantly amplified under the long-distance earthquake excitation, which needs to be considered in the design of similar structures in the future.

The displacement envelopes under the excitation of the Wenchuan earthquake calculated by the FE model for both directions are shown in Fig. 18. The maximum simulated displacements at the top floor are 0.156 and 0.057 m in directions *X* and *Y*, respectively. It is seen that the calculated displacements are larger in direction *X* than direction *Y*. The deformation curve is smooth without inflexions, similar to a deformed cantilever, indicating that the structure's deformations were remained in elastic stage under the seismic action.

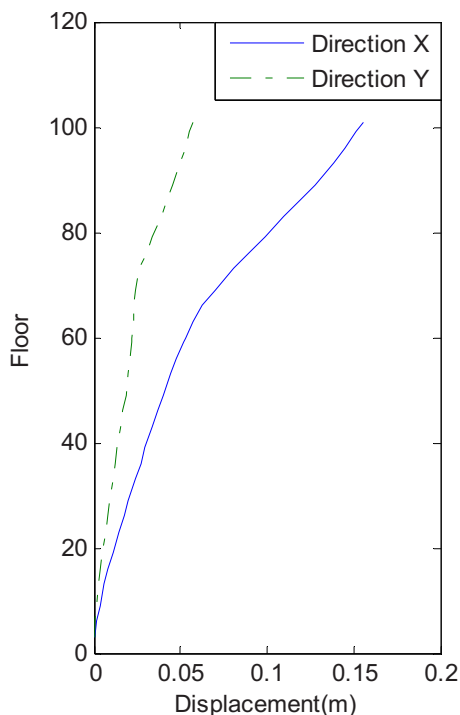


Fig. 18. Displacement envelope curves

Concluding Remarks

Through real-time monitoring of the structural acceleration responses of Taipei 101 Tower during three typhoons and under Wenchuan earthquake excitation, this paper presented selected results of the structural responses and dynamic behavior of the supertall building. Based on the detailed analysis of the measured data and numerical study, conclusions are summarized as follows:

1. The natural frequencies measured from Taipei 101 Tower during Typhoon Krosa and the Wenchuan earthquake were lower than those determined based on the measurements during Typhoons Matsa and Talim. This could be attributed to the differences of the vibration amplitudes of the tall building during the typhoons and the earthquake, indicating that the natural frequencies decreased as the vibration amplitude became larger.
2. The first sway mode shapes in the two orthogonal directions (directions *X* and *Y*) clearly demonstrate nonlinear variation with the building height. This is contrary to the assumption of a linear distribution for the first sway mode shape adopted in some codes and standards as well as in force measurements in wind tunnel tests for tall buildings.
3. The random decrement technique and the FDD method were used to estimate the damping ratios of the tall building. Reasonable agreement between the results by the two methods was observed. The damping ratios of the first sway mode in both directions were greater than those of the higher modes. The variations of the damping ratios with vibration amplitude were also noted. The relationship between the damping ratios and amplitude demonstrated nonlinear energy dissipation characteristics. Several damping curves reveal that the damping ratios increased with the increase of vibration amplitude. The measurement results showed that the fundamental modal damping ratios of 1.0–2.0% for lower vibration amplitudes (peak acceleration response < 10 mg) and 2–4% for higher vibration amplitudes (peak acceleration response > 10 mg) are reasonable for the wind-resistant analysis of the supertall building for serviceability consideration.
4. A 3D FE model was established for the numerical analysis of the supertall building. The calculated natural frequencies of the first several modes were compared with those determined from the field measurements. The differences between the calculated and measured natural frequencies for the first five modes were about 8.9–15.7%, and the measured results were larger than the calculated ones except the rotational mode. The MAC and NMD were used to measure the correlations between the measured and calculated sway mode shape vectors. The analysis results showed that there was a good correlation for Modes 1 and 2 in both directions, while the lower modes showed better correlations than the higher modes.
5. The dynamic responses of the supertall building under long-distance Wenchuan earthquake were investigated in detail. It was found that the majority of the high-frequency components of the excitation measured at the basement would have been filtered out by the earth during the long-distance travel. The amplitude spectral ratios or the transfer functions of the acceleration responses recorded at the 1st, 36th, 60th, 89th, and 101st floors to the base-mat acceleration showed significantly large amplifications at the identified structural modal frequencies. The rocking motions of the building were insignificant and could be ignored. The calculated acceleration responses matched those recorded by the accelerometers,

which illustrated that the dynamic analysis with the FEM can satisfactorily predict the seismic responses of the supertall building. The measured and calculated dynamic magnification factors demonstrated that the building was sensitive to dynamic excitations by such a long-distance earthquake. The calculated deformation curves were found to be smooth without inflexions, indicating that the structure still retained in elastic stage under the seismic action.

Acknowledgments

This work described in this paper was supported by a grant from the Research Grants Council of Hong Kong Special Administrative Region, China (Project No: CityU 116906). The writers are grateful to the owners and the management officials of Taipei 101 Tower for their supports and helps to the structural monitoring project. The writers wish to acknowledge the joint efforts of the staffs of the Central Weather Bureau of Taiwan who were involved in the establishment and development of the monitoring system. Thanks are due to Dr. Hong Fan for her contributions on the establishment of the FE model of Taipei 101 Tower.

References

Allemang, R. J., and Brown, D. L. (1982). "A correlation coefficient for modal vector analysis." *Proc., 1st Int. Modal Analysis Conf.*, Union College Press, Orlando, 110–116.

Andersen, P., Brincker, R., Peeters, B., and Roeck, G. D. (1999). "Comparison of system identification methods using ambient bridge test data." *Proc., 17th Int. Modal Analysis Conf.*, Vol. 3727, Society for Experimental Mechanics, Bethel, Conn., 1035–1041.

Bendat, J. S., and Piersol, A. G. (1993). *Engineering applications of correlation and spectral analysis*, 2nd Ed., Wiley, New York.

Brincker, R., Zhang, L., and Andersen, P. (2001). "Modal identification of output only systems using frequency domain decomposition." *Smart Mater. Struct.*, 10, 441–445.

Brownjohn, J. M. W. (2003). "Ambient vibration studies for system identification of tall buildings." *Earthquake Eng. Struct. Dyn.*, 32, 71–95.

Brownjohn, J. M. W., and Pan, T.-C. (2001). "Response of tall buildings to weak long distance earthquakes." *Earthquake Eng. Struct. Dyn.*, 30, 709–729.

Brownjohn, J. M. W., Pan, T. C., and Deng, X. Y. (2000). "Correlating dynamic characteristics from field measurements and numerical analysis of a high-rise building." *Earthquake Eng. Struct. Dyn.*, 29, 523–543.

Buildings Department of the Government of the Hong Kong SAR. (2004). *Code of practice on wind effects in Hong Kong*, Hong Kong.

Campbell, S., Kwok, K. C. S., Hitchcock, P. A., Tse, K. T., and Leung, H. Y. (2007). "Field measurements of natural periods of vibration and structural damping of wind-excited tall residential buildings." *Wind Struct.*, 10(5), 401–420.

Çelebi, M. (1993). "Seismic response of eccentrically braced tall building." *J. Struct. Eng.*, 119(4), 1188–1205.

Çelebi, M., and Şafak, E. (1992). "Seismic response of Pacific Park Plaza. I: Data and preliminary analysis." *J. Struct. Eng.*, 118(6), 1547–1565.

China Earthquake Administration. (2008). "Seismic parameters of Ms 8.0 earthquake at Wenchuan County of Sichuan Province." *China seismic information*, (http://www.csi.ac.cn/sichuan/sichuan080512_cs1.htm) (May 18, 2008) (in Chinese).

Ellis, B. R. (1980). "An assessment of the accuracy of predicting the fundamental natural frequencies of buildings and the implications concerning the dynamic analysis of structures." *Proc.-Inst. Civ. Eng.*, 69(3), 763–776.

Fan, H., Li, Q. S., Tuan, A. Y., and Xu, L. H. (2009). "Seismic analysis of the world's tallest building." *J. Constr. Steel Res.*, 65(5), 1206–1215.

Glanville, M. J., Kwok, K. C. S., and Denoon, R. O. (1996). "Full-scale damping measurements of structures in Australia." *J. Wind. Eng. Ind. Aerodyn.*, 59, 349–364.

Ivanovic, S. S., Trifunac, M. D., and Todorovska, M. I. (2000). "Ambient vibration tests of structures—A review." *ISSET J. Earthquake Technol.*, 37, 165–197.

Jeary, A. P. (1986). "Damping in tall buildings, a mechanism and a predictor." *Earthquake Eng. Struct. Dyn.*, 14, 733–750.

Kijewski, T., and Kareem, A. (2001). "Full-scale study of the behavior of tall buildings under winds." *Proc., SPIE Symp. on NDE for Health Monitoring and Diagnostics*, Bellingham, WA, 441–450.

Kim, B. H., Stubbs, N., and Park, T. (2005). "A new method to extract modal parameters using output-only responses." *J. Sound Vib.*, 282, 215–230.

Li, Q. S., et al. (2006). "Wind tunnel and full-scale study of wind effects on China's tallest building." *Eng. Struct.*, 28, 1745–1758.

Li, Q. S., Fang, J. Q., Jeary, A. P., and Wong, C. K. (1998). "Full scale measurement of wind effects on tall buildings." *J. Wind. Eng. Ind. Aerodyn.*, 74–76, 741–750.

Li, Q. S., and Wu, J. R. (2004). "Correlation of dynamic characteristic of a super tall building from full-scale measurements and numerical analysis with various finite element models." *Earthquake Eng. Struct. Dyn.*, 33(14), 1311–1336.

Li, Q. S., Xiao, Y. Q., and Wong, C. K. (2005). "Full-scale monitoring of typhoon effects on super tall buildings." *J. Fluids Struct.*, 20, 697–717.

Li, Q. S., Xiao, Y. Q., Wong, C. K., and Jeary, A. P. (2004). "Full-scale measurements of typhoon effects on a super tall building." *Eng. Struct.*, 26, 233–244.

Littler, J. D., and Ellis, B. R. (1992). "Full scale measurements to determine the response of Hume Point to wind loading." *J. Wind. Eng. Ind. Aerodyn.*, 42, 1085–1096.

Magalhaes, F., Cunha, A., Caetano, E., and Brincker, R. (2010). "Damping estimation using free decays and ambient vibration tests." *Mech. Syst. Signal Process.*, 24(5), 1274–1290.

Michel, C., Gueguen, P., and Bard, P.-Y. (2008). "Dynamic parameters of structures extracted from ambient vibration measurements: An aid for the seismic vulnerability assessment of existing buildings in moderate seismic hazard regions." *Soil Dyn. Earthquake Eng.*, 28, 593–604.

Ohkuma, T., Marukawa, H., Niihori, Y., and Kato, N. (1991). "Full-scale measurement of wind pressures and response accelerations of a high-rise building." *J. Wind. Eng. Ind. Aerodyn.*, 38, 185–196.

Pan, T. C. (1995). "When the doorbell rings—A case of building response to a long distance earthquake." *Earthquake Eng. Struct. Dyn.*, 24, 1343–1353.

Pan, T.-C., Brownjohn, J. M. W., and You, X. T. (2004). "Correlating measured and simulated dynamic responses of a tall building to long-distance earthquakes." *Earthquake Eng. Struct. Dyn.*, 33, 611–632.

Peeters, B., and Roeck, G. D. (2001). "Stochastic system identification for operational modal analysis: A review." *J. Dyn. Syst., Meas., Control*, 123, 659–667.

Pirnia, J. D., Kijewski-Correa, T., Abdelrazaq, A., Chung, J. Y., and Kareem, A. (2007). "Full-scale validation of wind-induced response of tall buildings: Investigation of amplitude-dependent properties." *Proc., 2007 Structures Congress*, Long Beach, Calif., 1–10.

Research Institute of Building and Construction. (2003). "Report on the structural design scheme of Taipei 101." *Rep. Prepared for Evergreen Consulting Engineering, Inc.*, Taipei, Taiwan.

Şafak, E., and Çelebi, M. (1992). "Recorded seismic response of Pacific Park Plaza. II: System identification." *J. Struct. Eng.*, 118(6), 1566–1589.

Standards Australia and Standards New Zealand. (2002). "Australian/New Zealand Standard, Structural design actions. Part 2: Wind actions." *AS/NZS 1170.2*, Australia/New Zealand.

Tamura, Y., Suda, K., and Sasaki, A. (2000). "Damping in buildings for

wind resistant design." *Proc., Int. Symp. on Wind and Structures for the 21st Century*, Techno Press, Yuseong-gu Daejeon, Korea, 115–130.

Tamura, Y., and Sugauma, S. (1996). "Evaluation of amplitude-dependent damping and natural frequency of buildings during strong winds." *J. Wind. Eng. Ind. Aerodyn.*, 59, 115–130.

Tamura, Y., Yoshida, A., and Zhang, L. (2005). "Damping in buildings

and estimation techniques." *Proc., 6th Asia-Pacific Conf. on Wind Engineering*, Techno Press, Yuseong-gu Daejeon, Korea, 193–214.

Tao, N. F., and Brownjohn, J. M. W. (1998). "Estimation of ground motion acceleration and building response to a long distance earthquake." *J. Earthquake Eng.*, 2(3), 477–485.

Waters, T. P. (1995). "Finite element model updating using measured frequency response functions." Ph.D. thesis, Univ. of Bristol, U.K.